Accepted Manuscript

Ammonium-iodide-salt additives induced photovoltaic performance enhancement in one-step solution process for perovskite solar cells

Y. Yang, J. Song, Y.L. Zhao, L. Zhu, X.Q. Gu, Y.Q. Gu, M. Che, Y.H. Qiang

PII: S0925-8388(16)31487-6

DOI: 10.1016/j.jallcom.2016.05.154

Reference: JALCOM 37674

To appear in: *Journal of Alloys and Compounds*

Received Date: 21 January 2016

Revised Date: 11 May 2016

Accepted Date: 15 May 2016

Please cite this article as: Y. Yang, J. Song, Y.L. Zhao, L. Zhu, X.Q. Gu, Y.Q. Gu, M. Che, Y.H. Qiang, Ammonium-iodide-salt additives induced photovoltaic performance enhancement in one-step solution process for perovskite solar cells, *Journal of Alloys and Compounds* (2016), doi: 10.1016/j.jallcom.2016.05.154.

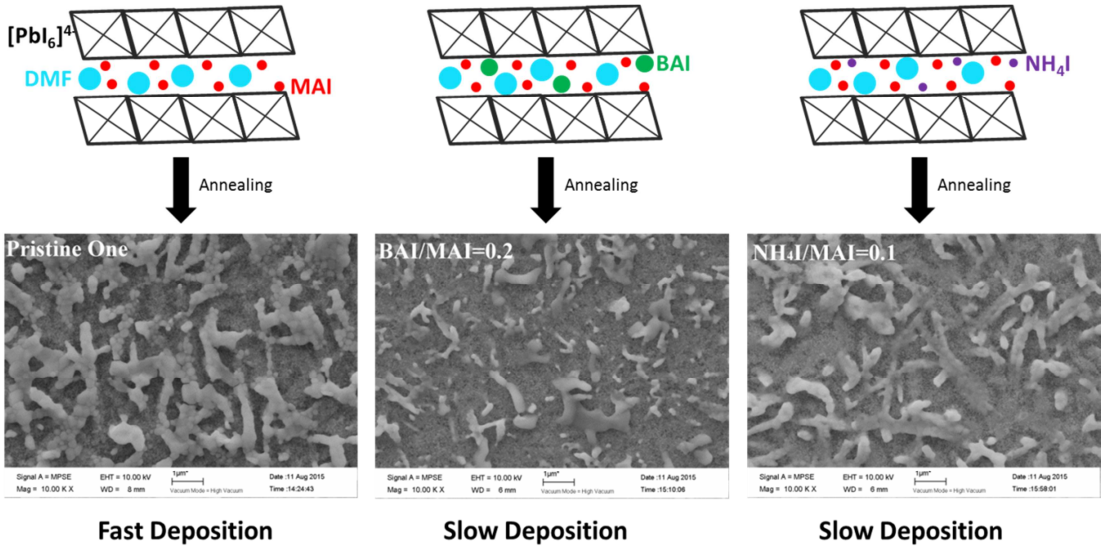

Fast Deposition **Slow Deposition** **Slow Deposition**

Ammonium-iodide-salt Additives Induced Photovoltaic Performance Enhancement in One-step Solution Process for Perovskite Solar Cells

Y. Yang, J. Song*, Y. L. Zhao, L. Zhu, X. Q. Gu, Y. Q. Gu, M. Che, Y. H. Qiang*

School of Materials Science and Engineering, China University of Mining and Technology, Xuzhou 221116, China

Abstract

Unordered aggregation of perovskite particles on TiO_2 mesoporous film surface is a common problem in one-step solution process for fabricating perovskite solar cells (PSCs). This phenomenon is harmful for homogeneous dispersion of perovskite in mesoporous TiO_2 film and responsible for the low photovoltaic performance of corresponding perovskite solar cells at the same time. Delicate control of perovskite nucleation and growth is an effective route to solve this problem. In this work, we proposed a facile strategy to improve perovskite ($CH_3NH_3PbI_3$) growth by adding $C_6H_5CH_2NH_3I$ (BAI) or NH_4I ionic compounds in perovskite precursor solution. We investigated perovskite crystal structure and morphology, optical and electrochemical properties of perovskite films or devices using different additives by XRD, SEM, UV-Vis, IPCE, and EIS. We found that these additives could decrease the grain size of perovskite crystal and diminish perovskite particle aggregation on TiO_2 film surface. This effect is benefit for electron transfer on perovskite/TiO_2 interface. Finally, perovskite solar cells using BAI or NH_4I additives obtain the best solar-to-electricity conversion efficiency of 9.05% and 9.49%, respectively, which are much higher than that of the pristine one, 6.83%.

***Keywords*:** Perovskite solar cells; Additives; One-step process; Crystal growth

* Corresponding authors

E-mail addresses: jsoong@cumt.edu.cn, yhqiang@cumt.edu.cn

1. Introduction

In the past few years, organic-inorganic lead halide perovskite based solar cells (PSCs) have become a research hotspot, and its power conversion efficiency has increased from 3% to as high as 20% [1-4], which is comparable to traditional photovoltaic devices, such as mc/a-Si, CdTe, etc. Organic-inorganic lead halide perovskite materials generally have suitable direct band gap (~ 1.5eV) [5], high light absorption coefficient (> 10^4 cm^{-1}) [5], fast electron and hole transfer rate, and long carrier transport length (100~1000 nm) by modulating its chemical composition [6-10]. All these superiorities make this material an outstanding light harvester for photovoltaic devices. Perovskite material is infiltrated in mesoporous TiO_2 film in conventional perovskite solar cells. Electron-hole pairs generated under light illumination in perovskite layer could be separated easily due to its low binding energy (~50 meV). Whilst, as the suitable energy level of TiO_2 and hole transfer materials (HTM) to $CH_3NH_3PbX_3$, electrons and holes could inject into TiO_2 layer and HTM layer, respectively, and finally they recombine in external circuit. Organic-inorganic lead halide perovskite film could be prepared by solution-processed and vapor-assisted techniques, such as one-step solution process [11], sequential deposition process [12], dual-source thermal evaporation process [13], vapor-assisted solution processes [14-16], and solvent post-treatment process [17], etc. In all these techniques, one-step solution method is the simplest and cheapest one, which has great potential in large-scale production.

It has been demonstrated that the morphology and crystallinity of perovskite films can significantly affect the photovoltaic properties of devices [12, 13, 18]. Unfortunately, perovskite film fabricated by one-step solution method usually presents inhomogeneous morphology [12]. The poor quality of perovskite layer would lead to low light harvesting, poor charge carrier mobility and lifetime, and even serious electron leakage. These disadvantages will induce low photovoltaic performance of the device [2]. Therefore, specific techniques are required for controlling perovskite crystal growth process. Additive-assisted method has been demonstrated to be an effective approach to improve perovskite layer morphology

[19-24]. By adding $PbCl_2$ or CH_3NH_3Cl in the perovskite precursor solution, the crystallinity of the resulting perovskite thin films could be enhanced greatly as the addition of Cl can slow down perovskite crystallization rate during the annealing process [6, 25, 26]. As a result, the mixed halide perovskites, $CH_3NH_3PbI_xCl_{3-x}$, present greatly improved photo-physical properties compared to those derived from pure iodide-based perovskite, especially in charge carrier diffusion process. HI additive in perovskite precursor solution could prohibit the decomposition of $CH_3NH_3PbI_3$ and obtain pure perovskite film without PbI_2 [27]. Solvent additives are also applied to modulate perovskite crystal process. The use of a mixed solvent of γ-butyrolactone and dimethylsulphoxide (DMSO) in perovskite precursor solution could form homogeneous perovskite films via a CH_3NH_3I–PbI_2–DMSO intermediate phase which is favorable for retarding the rapid reaction between PbI_2 and CH_3NH_3I [28].

In this work, we detailedly investigated the influence of benzylammonium iodide ($C_6H_5CH_2NH_3I$) and ammonium iodide (NH_4I) additives on $CH_3NH_3PbI_3$ crystallization behavior in one-step solution process. We found that the additives consisted of different cations had varied impacts on perovskite crystal formation. By adding proper amount of benzylammonium iodide or ammonium iodide, the efficiencies of corresponding perovskite solar cells increased by 33% and 39%, respectively, compared to the one without any additives.

2. Experimental Section

2.1. Synthesis of CH_3NH_3I and $C_6H_5CH_2NH_3I$

The methylammonium iodide (CH_3NH_3I, MAI) was synthesized in accordance with an early report [23]. Firstly, hydriodic acid (30 mL, 57 wt % aqueous solution, J&K) was slowly added into the methylamine solution (35 mL, 33 wt % in ethanol, J&K) in flowing N_2 atmosphere under stirring in an ice bath for 2 h. Afterward, the solution was rotary evaporated at 60 °C for 1 h. The resulting white precipitate was collected and re-dissolved in ethanol, and then recrystallized by adding diethyl ether in ethanol solution. The powder was re-dissolved and re-crystallized for three times. Finally, the

product was dried in vacuum at 60 °C overnight. The benzylammonium iodide ($C_6H_5CH_2NH_3I$, BAI) was synthesized by the similar process except replacing methylamine with benzylamine (20mL, 99%, J&K).

2.2. Preparation of perovskite precursor solution

To prepare the perovskite precursor solutions with or without additives, firstly, MAI (0.75 mmol) and PbI_2 (0.75 mmol, Sigma-Aldrich) powders were mixed in anhydrous dimethylformamide (DMF, 1.5 mL, J&K), and then $C_6H_5CH_2NH_3I$ or ammonium iodide (NH_4I, J&K) were added with molar rations of 0.05, 0.1, 0.2, and 0.3 to MAI. The final solutions were stirred at 70 °C until clear solutions were obtained, and they were filtered before using in perovskite thin-film deposition.

2.3. Cell fabrication

FTO-coated glass (15 Ω per square, Nippon Sheet Glass) with 20*20 mm size was etched by (Zn+HCl) solution to form two separated electrodes. The etched substrates were cleaned by ultrasonication in an alkaline aqueous washing solution, and then rinsed with deionized water, acetone, isopropanol, and ethanol, successively，as our early report [29]. After drying, a dense blocking layer of TiO_2 was deposited onto the substrate by spin-coating a TiO_2 colloid solution at 4500rpm for 30s and then calcinated at 450^{o}C for 1h. After cooling to room temperature, a mesoporous TiO_2 film was fabricated by spin-coating at 5000rpm for 30s using commercial TiO_2 paste (Dyesol 18NRT) which was diluted in ethanol (1:3.5, weight ratio). The film was prebaked at 100 ^{o}C for 30min, and then sintered at 500 ^{o}C for 1h in a muffle furnace. The prepared TiO_2 film was preheated at 70 ^{o}C before spin-coating perovskite precursor solutions. The perovskite film was deposited by spin-coating at 3000rpm for 30s using the prepared precursor solutions which were maintained at 70 ^{o}C during the whole procedure. After that, the perovskite film was heated at 100 ^{o}C for 30min. After cooling to room temperature, the hole transport material (HTM) layer was deposited by spin coating HTM solution at 3000 rpm for 30 s. The HTM solution was prepared by dissolving 72.3 mg (2,2’,7,7’-tetrakis(N,N-di-p-methoxyphenylamine)-9,9-spirobi-fluorene) (spiro-MeOTAD), 28.8μL 4-tert-butylpyridine (TBP), 17.5 μL of bis(trifluoromethylsulphonyl)imide (LiTFSI) in acetonitrile (520 mg/mL) in 1 mL

chlorobenzene. After standing at dried air over night, 80nm of silver was thermally evaporated on top of the device to form the back contact.

2.4. Characterization

The structure and morphology of the as-prepared films were measured by X-ray diffraction (XRD, D8 ADVANCE, Bruker), scanning electron microscopy (SEM, 1530VP, LEO). The photo-absorption properties of different perovskite films are characterized by UV-Vis spectrophotometer (CARY 300 Conc). Photocurrent–voltage (*J–V*) characteristic curves of PSCs were recorded by an electrochemical workstation (Keithley, 2420 Source Meter). The cell was illuminated by a solar simulator (Oriel Sol 3A, Newport) under 100 $mW \cdot cm^{-2}$ irradiation, calibrated by a standard silicon solar cell (Oriel Instrument). A non-reflective metal aperture of 0.1 cm^2 was used to define the active area of the device and avoid light scattering through the sides. The scan range was 1.0V to 0V. Electrochemical impedance spectroscopy (EIS) was recorded using IM6ex electrochemical workstation. EIS spectra were measured in dark, and the frequency range was from 100 kHz to 100 mHz with an AC modulation signal of 10 mV and bias DC voltage of 0.60 V. The IPCE was measured using a power source (Newport 300W Xenon lamp, 66902) with a monochromator (Newport Cornerstone 260) and a power meter (Newport 2936-C).

3. Results and Discussion

3.1 Microstructure and optical property of perovskite films

XRD patterns of different perovskite films are shown in Fig. 1. For the pristine perovskite film, peaks at 13.9°, 19.8°, 28.2°, 31.7°, 40.4°, and 42.8° are in good agreement with the tetragonal phase of the $CH_3NH_3PbI_3$ perovskite [28, 30], corresponding lattice plane are marked in Fig. 1a. The sharp diffraction peaks indicate that perovskite film has good crystallization. As the addition of BAI, the most remarkable change is the variation of peak strength at 13.9°. For perovskite film using BAI/MAI of 0.05, corresponding diffraction peaks are similar to the pristine one. However, as BAI/MAI ratio increases, the peak at 13.9° turns weak and wide. The relatively low diffraction intensity indicates small sized perovskite grains or poor

crystallization. In the case of perovskite films using NH_4I additive, the diffraction peaks turn weak a little as the increase amount of NH_4I additive, but they are relatively sharper even when NH_4I/MAI is up to 0.3 than BAI based perovskite films. This result indicates that NH_4I presents weaker influence on $CH_3NH_3PbI_3$ perovskite growth compared to BAI. The varied impact of BAI and NH_4I on perovskite growth may be induced by the larger ion size of BA^+ than NH_4^+.

The scanning electron microscopy (SEM) is employed to observe surface morphology of different perovskite films. As shown in Fig. 2, for the pristine perovskite film without any additives, perovskite nanoparticles aggregate into irregular rods and scatter on TiO_2 film. The morphologies of perovskite films are similar to the pristine one when additive of BAI or NH_4I are few (BAI/MAI=0.05-0.1 and NH_4I/MAI=0.05-0.2), except that the density of perovskite rods on TiO_2 film reduce slightly. When BAI/MAI ratio increases to 0.2, perovskite rods are cracked into different sizes of pieces with relatively poor crystallization. As BAI/MAI ratio increases further to 0.3, small perovskite particles gather densely. In regard to NH_4I additive, large perovskite rods disappear and particle aggregations arise when NH_4I/MAI ratio reaches to 0.3. Briefly, BAI and NH_4I additives could diminish the size of perovskite particles on TiO_2 surface while weaken crystallinity of perovskite films. This morphology transformation concurs with XRD patterns above. In fact, pristine perovskite film with well-crystalline is formed due to the strong ionic interactions under evaporation and convective process during spinning. BA^+ and NH_4^+ in precursor solution would intercalate between $CH_3NH_3^+$ and $[PbI_6]^{4-}$ and prevent the fast deposition of $CH_3NH_3PbI_3$. The slow deposition process could suppress agglomeration of perovskite grains, but reduce crystallization quality of perovskite in the subsequent heat procedure. From XRD and SEM results, we find that BAI present stronger ability in surpressing crystallization process of perovskite than NH_4I additive. It might derive from the larger size of BA^+ than NH_4^+.

Fig. 3 shows the UV−vis absorption spectra of the perovskite films processed with or without additives. Apparently, the perovskite films based on BAI additive have higher absorbance than the pristine one. Usually, high coverage and continuous

perovskite crystalline film could absorb more sunlight. However, we could see from SEM images that coverage of perovskite crystalline films did not increase as the addition of BAI. On the contrary, the surface coverage of perovskite films decrease as the addition of BAI arised from 0.05 to 0.3. These results demonstrate that the increased light absorbance should not be induced by improvement of perovskite film coverage. In our opinion, the enhanced light absorbance may be attributed to the better penetration of smaller perovskite grains in TiO_2 porous film. In the case of perovskite films based on NH_4I additive, light absorbance is close to each other under different amount of additive. It could be attributed to the unconspicuous change of perovskite crystal according to XRD results. However, the light absorbance is enhanced greatly in the long wavelength ranging from 550 to 750 nm. In fact, light absorbance enhancement of perovskite film is the prerequisite for a high short-circuit current in perovskite solar cells.

3.2 Photovoltaic performance of perovskite solar cells

The *J-V* curves of different devices are shown in Fig. 4, and the corresponding photovoltaic performance parameters are summarized in Table 1. The pristine perovskite solar cell exhibits a conversion efficiency of 6.83% with *Jsc* of 11.51 mA/cm^2, *Voc* of 0.85 V, and *FF* of 0.70. As BAI is introduced in perovskite precursor solution, corresponding devices show significant improvement in *Jsc*. The BAI additive based devices achieve the best photovoltaic performance when BAI/MAI is 0.2, presenting a conversion efficiency of 9.05% with *Jsc* of 14.61 mA/cm^2, *Voc* of 0.86 V, and *FF* of 0.72. Perovskite morphology optimization and light absorption enhancement owing to BAI addition are the main reasons for photovoltaic property improvement of the device. However, when BAI/MAI reaches to 0.3, conversion efficiency of the device drop down dramatically to 7.84%, although the perovskite film has high performance in light absorbance. This could be induced by the poor crystallization of perovskite and residual impurity of BAI in perovskite film. For NH_4I additive based devices, the photovoltaic properties are enhanced when increasing NH_4I/MAI from 0 to 0.1, but declined as NH_4I/MAI is raised further to 0.3.

The best performance is obtained when NH_4I/MAI is 0.1 with *Jsc* of 15.31 mA/cm^2, *Voc* of 0.86 V, *FF* of 0.72, and conversion efficiency of 9.49%. Compared to BAI additive based PSCs, these devices present relatively higher *Jsc*, deriving from their larger absorption in long wavelength region and comparable crystallinity to the pristine one. Finally, perovskite solar cell using optimal amount of NH_4I additive has relatively higher photovoltaic performance than that based on BAI additive.

The incident photon-to-current conversion efficiency (IPCE) spectra are shown in Fig. 5. The onset of photocurrent at 800 nm is consistent with the band gap of $CH_3NH_3PbI_3$ (~1.5 eV). The pristine device presents conversion efficiency from 45% to 65% in the range of 400-700 nm. As BAI additive is introduced in precursor solution, the quantum efficiency increase evidently. When BAI/MAI reaches to 0.2, corresponding devices show the highest quantum efficiency, which is in accordance with its highest *Jsc* value. For NH_4I addtive based devices, similar results are proceeded. However, quantum efficiency reduces more slowly from 450 nm to 700 nm for NH_4I addtive based devices than BAI additive based devices and the pristine one. This result should be attributed to the relatively stable absorbance of perovskite films using NH_4I additive from 550 nm to 750 nm, as shown in UV-Vis spectra. Besides, we could see that quantum yield of perovskite solar cells do not always coincide with light absorption strength of corresponding perovskite films from UV-Vis and IPCE results. For example, perovskite film with BAI/MAI=0.3 exhibits the highest absorbance in all the perovskite films, but the corresponding solar cell presents a relative lower performance than the film using BAI/MAI=0.2. In fact, quantum yield of solar cells concerns not only light harvesting of active layer but also charge transfer process both in perovskite film and on TiO_2/perovskite or perovskite/HTM interfaces. As demonstrated in Fig. 1, perovskite film with BAI/MAI=0.3 presents poor crystallinity, which is bad for the charge transfer in perovskite film.

3.3 Electrochemical property of perovskite solar cells

To investigate the electrochemical properties of interfaces with or without different

additive treatments, electrochemical impedance spectrometry (EIS) of the pristine cell, BAI and NH_4I based cells with the highest photovoltaic performance are conducted under dark conditions with a bias voltage of 0.6 V in this work. As shown in Fig. 6, Nyquist plots are usually composed of two irregular semicircles, including the small one at high frequency and the large one at low frequency [31-33]. The equivalent circuit is inserted in Fig. 6. The value of the starting point at the real part of the Nyquist plot corresponds to the series resistance Rs. Rs is mainly related to the resistance of FTO substrate [34, 35]. The first semicircle is attributed to the resistance (R1) of hole transporting on the HTM/perovskite interface. The second semicircle in the low frequency range is associated with the recombination resistance (R2) at the TiO_2/perovskite interface, a large R2 value indicates a hard recombination. The devices with or without additive treatments exhibit a similar resistance Rs and R1. The main difference of perovskite devices lies in R2. It could be observed that both BAI additive-based and NH_4I additive-based perovskite devices present a much higher resistance (R2) than the pristine one. The increased resistance will retard charge recombination at TiO_2/perovskite interface. Because of the low recombination rate at TiO_2/perovskite interface, it is reasonable that additive-based PSCs show a higher *Jsc* and V_{OC} than that of the pristine one [36].

In fact, the decreased recombination rate at TiO_2/perovskite interface is closely related to morphology modification of perovskite film in the device. BAI additive could diminish perovskite grains and further enhance the infiltration process of perovskite in TiO_2 pores. This modification would improve the interaction between perovskite and TiO_2 particles and promote the charge transfer in TiO_2/perovskite interface. For NH_4I based perovskite film, perovskite grains present relatively smaller changes in size compared to BAI. This result may be the main reason that NH_4I based perovskite solar cells have a smaller recombination resistance (R2) on TiO_2/perovskite interface than BAI based one. The light absorption enhancement of NH_4I based perovskite films in long wavelength is the main reason for their high photovoltaic performance.

4. Conclusion

We presented a facile procedure to improve the photovoltaic performance of perovskite solar cell by introducing BAI or NH_4I additives in perovskite precursor solution in one-step solution process. Proper amount of BAI or NH_4I additives in precursor solution was crucial for perovskite crystallization and growth in TiO_2 porous film. The devices showed the best performance when the molar ratio of BAI/MAI and NH_4I/MAI were 0.2 and 0.1, respectively. Perovskite films fabricated under assistance of these additives presented better light harvesting property and low charge recombination at perovskite/TiO_2 interface. Finally, BAI or NH_4I additives based perovskite solar cells obtained solar-to-electricity conversion efficiency of 9.05% and 9.49%, respectively, which were higher than that of the pristine one, 6.83%.

Acknowledgments

This work was supported by the Fundamental Research Funds for the Central Universities (2015XKZD01).

Reference

[1] A. Kojima, K. Teshima, Y. Shirai, T. Miyasaka, Organometal halide perovskites as visible-light sensitizers for photovoltaic cells, J. Am. Chem. Soc. 131(2009) 6050-6051.

[2] H. S. Kim, C. R. Lee, J. H. Im, K. B. Lee, T. Moehl, A. Marchioro, S. J. Moon, R. Humphry-Baker, J. H. Yum, J. E. Moser, M. Grätzel, N. G. Park, Lead iodide perovskite sensitized all-solid-state submicron thin film mesoscopic solar cell with efficiency exceeding 9%, Sci. Rep. 2 (2012) 591-597.

[3] W. S. Yang, J. H. Noh, N. J. Jeon, Y. C. Kim, S. Ryu, J. Seo, S. II Seok, High-performance photovoltaic perovskite layers fabricated through intramolecular exchange, Science 348 (2015) 1234-1237.

[4] W. Chen, Y. Z. Wu, Y. F. Yue, J. Liu, W. J. Zhang, X. D. Yang, H. Chen, E. B. Bi, I. Ashraful, M. Grätzel, L. Y. Han, Efficient and stable large-area perovskite solar cells with inorganic charge extraction layers, Science 350 (2015) 944-948.

[5] S. De Wolf, J. Holovsky, S.-J. Moon, P. Löper, B. Niesen, M. Ledinsky, F.-J. Haug, J.-H. Yum, C. Ballif, Organometallic halide perovskites: sharp optical absorption edge and its relation to photovoltaic performance, J. Phys. Chem. Lett. 5 (2014) 1035-1039.

[6] M. M. Lee, J. Teuscher, T. Miyasaka, T. N. Murakami, H. J. Snaith, Efficient hybrid solar cells based on meso-superstructured organometal halide perovskites, Science 338 (2012) 643-647.

[7] G. Xing, N. Mathews, S. Sun, S. S. Lim, Y. M. Lam, M. Grätzel, S. Mhaisalkar, T. C. Sum, Long-range balanced electron- and hole-transport lengths in organic-inorganic $CH_3NH_3PbI_3$, Science 342 (2013) 344-347.

[8] S. D. Stranks, G. E. Eperon, G. Grancini, C. Menelaou, M. J. Alcocer, T. Leijtens, L. M. Herz, A. Petrozza, H. J. Snaith, Electron-hole diffusion lengths exceeding 1 micrometer in an organometal trihalide perovskite absorber, Science 342 (2013) 341-344.

[9] Y. Zhao, A. M. Nardes, K. Zhu, Solid-State mesostructured perovskite $CH_3NH_3PbI_3$ solar cells: charge transport, recombination, and diffusion length, J. Phys. Chem. Lett. 5 (2014) 490-494.

[10] P. Bhatt, K. Pandey, P. Yadav, B. Tripathi, P. C. Kanth, M. K. Pandey, M. Kumar, Investigating the charge carrier transport within the hole-transport material free perovskite solar cell processed in ambient air, Sol. Energy Mater. Sol. Cells 140 (2015) 320-327.

[11] M. J. Carnie, C. Charbonneau, M. L. Davies, J. Troughton, T. M. Watson, K. Wojciechowski, H. Snaith, D. A. Worsley, A one-step low temperature processing route for organolead halide perovskite solar cells, Chem. Commun. 49 (2013) 7893-7895.

[12] J. L. Burschka, N. Pellet, S. -J. Moon, R. Humphry-Baker, P. Gao, M. K. Nazeeruddin, M. Grätzel, Sequential deposition as a route to high-performance perovskite-sensitized solar cells, Nature 499 (2013) 316-319.

[13] M. Z. Liu, M. B. Johnston, H. J. Snaith, Efficient planar heterojunction perovskite solar cells by vapour deposition, Nature 501 (2013) 395-398.

[14] Q. Chen, H. P. Zhou, Z. R. Hong, S. Luo, H. S. Duan, H. H. Wang, Y. S. Liu, G. Li, Y. Yang, Planar heterojunction perovskite solar cells via vapor-assisted solution process, J. Am. Chem. Soc. 2 (2014) 622-625.

[15] S. Casaluci, L. Cina, A. Pockett, P. S. Kubiak, R. G. Niemann, A. Reale, A. Di Carlo, P. J. Cameron, A simple approach for the fabrication of perovskite solar cells in air, J. Power Sources 297 (2015) 504-510.

[16] Z. G. Xiao, Q. F. Dong, C. Bi, Y. C. Shao, Y. B. Yuan, J. S. Huang, Solvent annealing of perovskite-induced crystal growth for photovoltaic-device efficiency enhancement, Adv. Mater. 26 (2014) 6503-6509.

[17] K. F. Lin, S. H. Chang, K. H. Wang, H. M. Cheng, K. Y. Chiu, K. M. Lee, S. H. Chen, C. G. Wu, Unraveling the high performance of tri-iodide perovskite absorber based photovoltaics with a non-polar solvent washing treatment, Sol. Energy Mater. Sol. Cells 141 (2015) 309-314.

[18] Y. Zhao, J. Liu, X. R. Lu, Y. D. Gao, X. Z. You, X. X. Wu, Improving the efficiency of perovskite solar cells through optimization of the $CH_3NH_3PbI_3$ film growth in solution process method, Appl. Surf. Sci. 359 (2015) 560-566.

[19] C. T. Zuo, L. M. Ding, An 80.11% FF record achieved for perovskite solar cells by using the NH_4Cl additive, Nanoscale 6 (2014) 9935-9938.

[20] J. Zhang, Z. L. Hu, L. K. Huang, G. Q. Yue, J. W. Liu, X. W. Lu, Z. Y. Hu, M. H. Shang, L. Y. Han, Y. J. Zhu, Bifunctional alkyl chain barriers for efficient perovskite solar cells, Chem. Commun. 51 (2015) 7047-7050.

[21] Y. T. Shi, X. Y. Wang, H. Zhang, B. Li, H. L. Lu, T. L. Ma, C. Hao, Effects of 4-tert-butylpyridine on perovskite formation and performance of solution-processed perovskite solar cells, J. Mater. Chem A 3 (2015) 22191-22198.

[22] C. C. Chueh, C. Y. Liao, F. Zuo, S. T. Williams, P. W. Liang, A. K.-Y. Jen, The roles of alkyl halide additives in enhancing perovskite solar cell performance, J. Mater. Chem A 3 (2015)

9058-9062.

[23] C. Y. Chang, C. Y. Chu, Y. C. Huang, C. W. Huang, S. Y. Chang, C. A. Chen, C. Y. Chao, W. F. Su, Tuning perovskite morphology by polymer additive for high efficiency solar cell, ACS Appl. Mater. Inter. 7 (2015) 4955-4961.

[24] J. Cao, J. Yin, S. F. Yuan, Y. Zhao, J. Li, N. F. Zheng, Thiols as interfacial modifiers to enhance the performance and stability of perovskite solar cells, Nanoscale 7 (2015) 9443-9447.

[25] J. M. Ball, M. M. Lee, A. Hey, H. J. Snaith, Low-temperature processed meso-superstructured to thin-film perovskite solar cells, Energy Environ. Sci. 6 (2013) 1739-1743.

[26] Y. Zhao, K. Zhu, CH_3NH_3Cl-assisted one-step solution growth of $CH_3NH_3PbI_3$: structure, charge-carrier dynamics, and photovoltaic properties of perovskite solar cells. J. Phys. Chem. C 118 (2014) 9412-9418.

[27] J. H. Heo, D. H. Song, H. J. Han, S. Y. Kim, J. H. Kim, D. Kim, H. W. Shin, T. K. Ahn, C. Wolf, T. W. Lee, S. H. Im, Planar $CH_3NH_3PbI_3$ perovskite solar cells with constant 17.2% average power conversion efficiency irrespective of the scan rate, Adv. Mater. 27 (2015) 3424-3430.

[28] N. J. Jeon, J. H. Noh, Y. C. Kim, W. S. Yang, S. C. Ryu, S. II Seok, Solvent engineering for high-performance inorganic-organic hybrid perovskite solar cells, Nat. Mater. 13 (2014) 897-903.

[29] X. P. Lin, D. M. Song, X. Q. Gu, Y. L. Zhao, Y. H. Qiang, Synthesis of hollow spherical TiO_2 for dye-sensitized solar cells with enhanced performance, Appl. Surf. Sci. 263 (2012) 816-820.

[30] T. Baikie,Y. N. Fang, J. M. Kadro, M. Schreyer, F. X. Wei, S. G. Mhaisalkar, M. Grätzel, T. J. White, Synthesis and crystal chemistry of the hybrid perovskite $(CH_3NH_3)PbI_3$ for solid-state sensitized solar cell applications, J.Mater.Chem. A 1 (2013) 5628-5641.

[31] V. Gonzalez-Pedro, E. Juarez-Perez, W. Arsyad, E. Barea, F. Fabregat-Santiago, I. Mora-Sero, J. Bisquert, General working principles of $CH_3NH_3PbX_3$ perovskite solar cells, Nano Lett. 14 (2014) 888-893.

[32] E. Juarez-Perez, M. Wuβler, F. Fabregat-Santiago, K. Lakus-Wollny, E. Mankel, T. Mayer, W. Jaegermann, I. Mora-Sero, Role of the selective contacts in the performance of lead halide perovskite solar cells, J. Phys. Chem. Lett. 5 (2014) 680-685.

[33] H. S. Kim, J. W. Lee, N. Yantara, P. P. Boix, S. A. Kulkarni, S. Mhaisalkar, M. Grätzel, N. G. Park, High efficiency solid-state sensitized solar cell-based on submicrometer rutile TiO_2 nanorod and $CH_3NH_3PbI_3$ perovskite sensitizer, Nano Lett. 13 (2013) 2412-2417.

[34] G. D. Niu, W. Z. Li, F. Q. Meng, L. D. Wang, H. P. Dong, Y. Qiu, Study on the stability of $CH_3NH_3PbI_3$ films and the effect of post-modification by aluminum oxide in all-solid-state hybrid solar cells, J. Mater. Chem. A 2 (2014) 705-708.

[35] Y. L. Zhao, X. Q. Gu, Y. H. Qiang, Influence of growth time and annealing on rutile TiO_2 single-crystal nanorod arrays synthesized by hydrothermal method in dye-sensitized solar cells, Thin Solid Films 520 (2012) 2814-2818.

[36] K. Wang, Y. T. Shi, Q. S. Dong, Y. Li, S. F. Wang, X. F. Yu, M. Y. Wu, T. L. Ma, Low-temperature and solution-processed amorphous WOx as electron-selective layer for perovskite solar cells, J. Phys. Chem. Lett. 6 (2015) 755-759.

Figure captions

Fig. 1 XRD patterns of perovskite films using different amounts of BAI (a) or NH_4I (b) additives.

Fig.2 SEM images of pristine perovskite film or films with BAI and NH_4I additives. The values mean molar ratio of BAI/MAI or NH_4I/MAI. The scale bars are 1μm.

Fig. 3 UV-Visible absorption spectra of different perovskite films based on BAI additive (a) and NH_4I additive (b).

Fig. 4 Current density−voltage curves of devices with different amounts of BAI (a) or NH_4I (b) additives in the perovskite films. All the devices were measured under illumination of 100 mW/cm^2 and active area of $0.1cm^2$.

Fig. 5 IPCE spectra of perovskite devices based on BAI additive (a) and NH_4I additive (b).

Fig. 6 Nyquist plots of PSCs based on pristine perovskite film, and films with BAI (BAI/MAI=0.2) or NH_4I additive (NH_4I/MAI=0.1) in dark at 0.6 V. The inset is corresponding equivalent circuit.

Table caption

Table 1 Photovoltaic parameters of perovskite solar cells based on different additives in perovskite films. *Jsc*, *Voc*, *FF*, and η represent short-circuit current density, open-circuit voltage, fill factor, and conversion efficiency, respectively.

Samples	J_{sc} (mA·cm^{-2})	V_{oc} (V)	FF	η (%)
Pristine One	11.51	0.85	0.70	6.83
BAI/MAI=0.05	12.26	0.83	0.70	7.18
BAI/MAI=0.1	13.41	0.85	0.72	8.11
BAI/MAI=0.2	14.61	0.86	0.72	9.05
BAI/MAI=0.3	13.67	0.86	0.70	7.84
NH_4I/MAI=0.05	13.24	0.86	0.69	7.91
NH_4I/MAI=0.1	15.31	0.86	0.72	9.49
NH_4I/MAI=0.2	14.86	0.83	0.71	8.69
NH_4I/MAI=0.3	12.83	0.84	0.70	7.54

Table 1

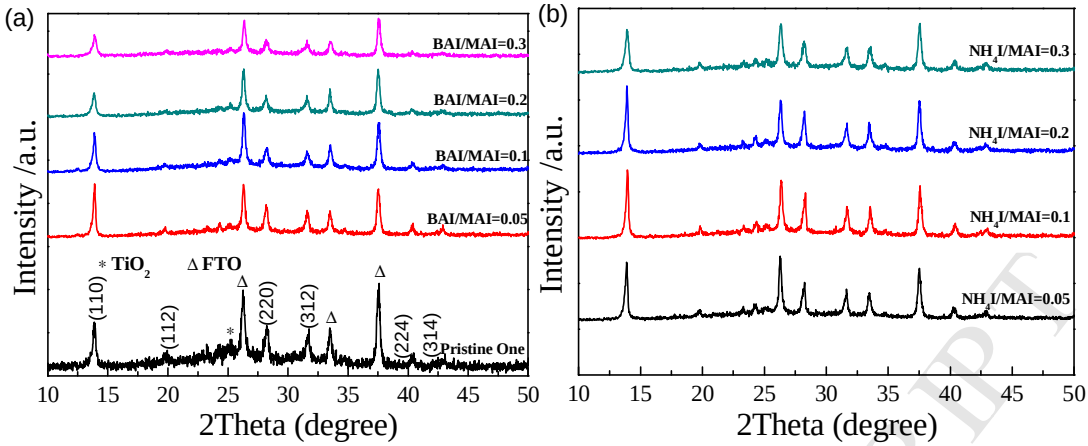

Fig. 1

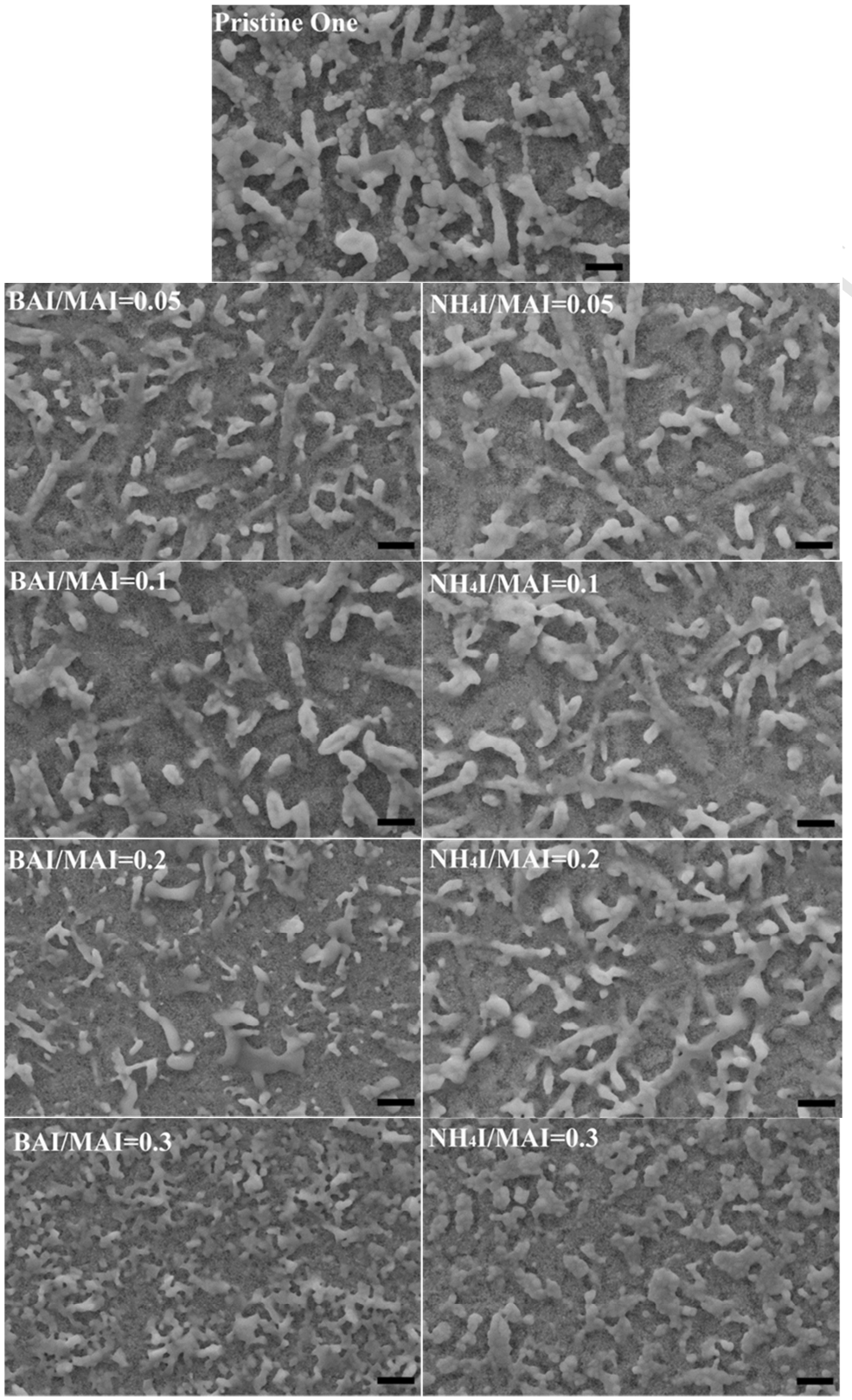
Pristine One
BAI/MAI=0.05
NH4I/MAI=0.05
BAI/MAI=0.1
NH4I/MAI=0.1
BAI/MAI=0.2
NH4I/MAI=0.2
BAI/MAI=0.3
NH4I/MAI=0.3

Fig. 2

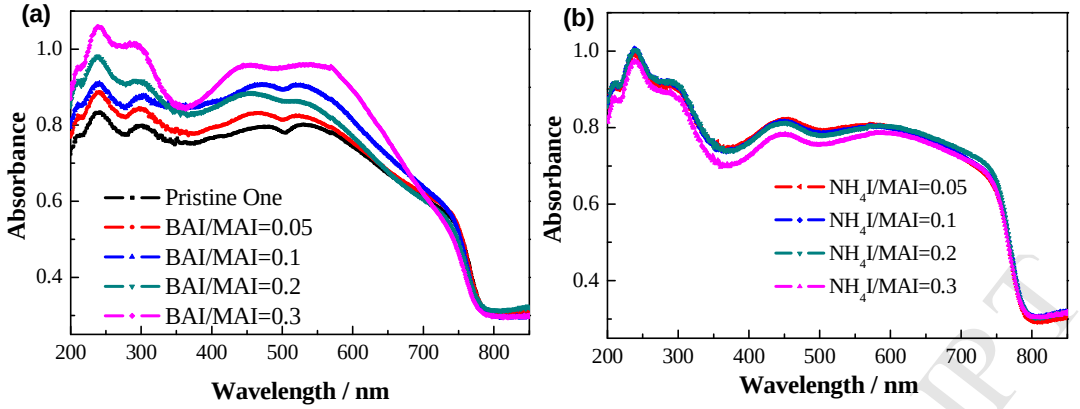

Fig. 3

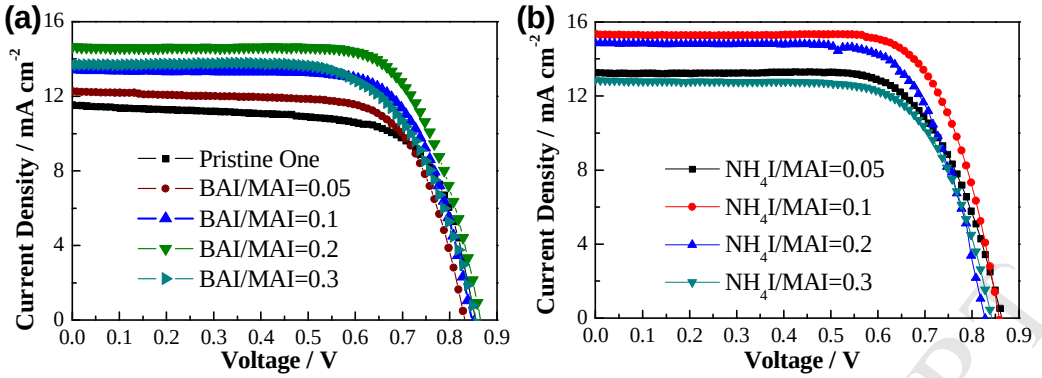

Fig. 4

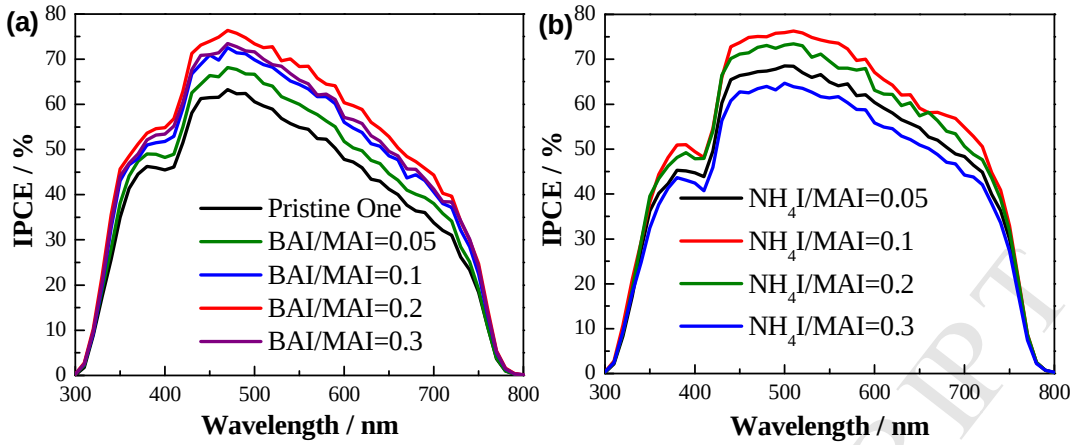

Fig. 5

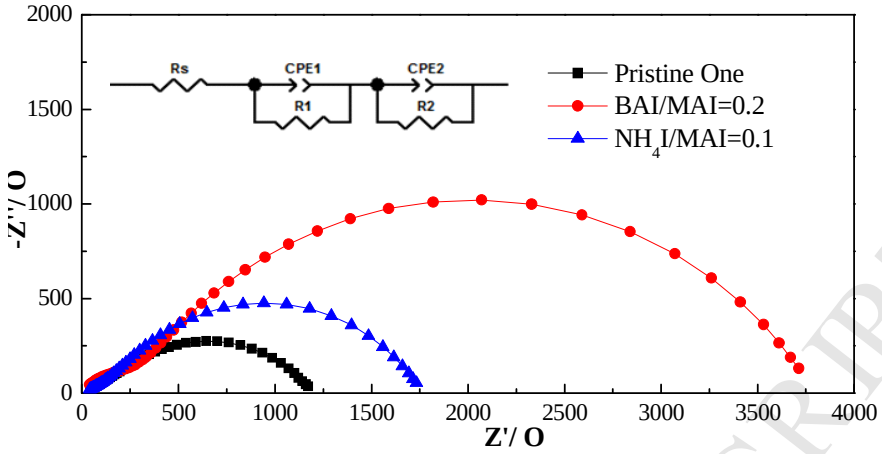

Fig. 6

Highlights

1. Perovskite films were deposited in one-step solution process using BAI and NH_4I additives

2. Photovoltaic performance increased by 33% and 39% for BAI and NH_4I additive based perovskite solar cells compared to the pristine one

3. BAI and NH_4I additive could improve perovskite morphology and perovskite/TiO_2 interface